

We are IntechOpen, the world's leading publisher of Open Access books Built by scientists, for scientists

6,900

Open access books available

186,000

International authors and editors

200M

Downloads

Our authors are among the

154

Countries delivered to

TOP 1%

most cited scientists

12.2%

Contributors from top 500 universities



WEB OF SCIENCE™

Selection of our books indexed in the Book Citation Index
in Web of Science™ Core Collection (BKCI)

Interested in publishing with us?
Contact book.department@intechopen.com

Numbers displayed above are based on latest data collected.
For more information visit www.intechopen.com



Concepts and Components for Pulsed Angle Modulated Ultra Wideband Communication and Radar Systems

Alexander Esswein, Robert Weigel, Christian Carlowitz and Martin Vossiek

Additional information is available at the end of the chapter

<http://dx.doi.org/10.5772/55082>

1. Introduction

Ultra Wideband (UWB) systems have been utilized and commercialized since the beginning of the 1970s and have been successfully used in ground-, wall- and foliage-penetration, collision warning and avoidance, fluid level detection, intruder detection and vehicle radar and also for the topics of the intended research project, communication and position-location [1]. Up to now, the latter two fields have been treated separately in most developments.

UWB has the potential to yield solutions for the challenging problem of time dispersion caused by multipath propagation in indoor channels. For a local positioning system, multipath propagation determines the physical limit of the maximal accuracy that can be obtained at a given signal bandwidth [14].

There exist several techniques which are used to generate ultra wideband signals. Traditionally, UWB was defined as pulse based radio. Especially for radar and localization applications, the use of very narrow pulses is still the most dominant technique. In addition to that, there are UWB systems that use more complex modulation techniques, like multiband orthogonal frequency-division multiplexing (MB-OFDM) or direct sequence code-division multiple access (DS-CDMA) to spread the transmitted information over a large bandwidth. They are applied in communication systems whereas radar systems that use such techniques can hardly be found.

Recently there can be recognized an increasing interest for UWB technologies applied in mm-wave frequency bands. This interest is stimulated by novel regulation for future vehicular UWB systems in the 79 GHz band (77 - 81 GHz) [12], novel international allocation of unlicensed bands ranging from 57 - 66 GHz [9] and the attractive ISM bands at 122.5 GHz with 1 GHz bandwidth and at 244 GHz with 2 GHz bandwidth. Also, the 61.5 GHz ISM band with 500 MHz available bandwidth is often considered as a “de-facto” UWB band even though the bandwidth is just less than the bandwidth of 500 MHz usually demanded as the minimal bandwidth for UWB. The great advantage of mm-wave UWB bands is that they do not suffer from the severe power regulations known from standard UWB. At the above

mentioned mm-wave UWB bands, the permitted maximum mean power density is at least 38 dB higher than in the UWB bands below 30 GHz.

Most of the mm-wave UWB communication and ranging systems published so far use a simple pulse generator as signal source. In the simplest case, a mm-wave CW carrier is modulated with an ASK (s. e.g [17]) or BPSK (s. e.g. [18]) sequence. A very interesting low-power approach that is somewhat related to the approach in this work is shown in [6] and [7]. Here, a 60 GHz oscillator itself is switched on and off. To guarantee a stable startup phase and to improve the phase noise, the oscillator is injection locked to a spurious harmonic of the switching signal. The benefit of the pulsed injection locking approach with respect to power consumption was impressively shown in this work. The general approach to obtain a stable pulse to pulse phase condition by injecting a spurious harmonic of the switching pulse into the oscillator is well known for a long time from low-power and low-cost microwave primary pulse radar systems. This basic principle can be extended in a way that frequency modulated signals can be generated based on a switched injection locked oscillator [19]. In this work, it is generalized for synthesizing arbitrarily phase modulated signals for integrated local positioning and communication. The fusion of positioning and communication capability is especially needed for future wireless devices applied in the "internet of things" or for advanced multimedia / augmented reality applications, for robot control and for vehicle2X / car2X applications.

Most existing UWB communication and ranging systems - especially those dedicated to low power consumption and mm-wave frequencies - employ simple impulse radios (IR). Popular IR-UWB modulation techniques include on-off keying (OOK), pulse-position modulation (PPM), pulse-amplitude modulation (PAM) and binary phase shift keying (BPSK) [5, 17, 18]. Their waveform can be synthesized using low complexity impulse generators and control circuitry, which comes at the cost of low spectral efficiency and severely limited control over spectral properties of the synthesized signals. Consequently, these transmitter cannot exhaust regulatory boundaries in all operation modes. High data rate synthesizers are often average power limited whereas low data rate implementations may be peak power limited [20].

2. Proposed concepts and components

In order to overcome these issues, pulsed angle modulated UWB signals are proposed to provide greater flexibility and better control over the spectral properties of the synthesized signals. Additionally, this signal type is well suited for both ranging and communication, since it allows synthesizing pulsed frequency modulated chirps that are attractive for ranging as well as digital phase modulation schemes for data transmission with the same hardware.

Since classic architectures containing VCOs, PLLs, mixer, linear amplifiers and switches are not suited for low complexity, low power systems, the switched injection-locked oscillator is suggested for signal synthesis. It regenerates and amplifies a weak phase-modulated signal. Consequently, the high frequency RF signal can be generated from a high power but efficiently synthesized low frequency phase modulated baseband signal in two simple stages - a lossy passive or low power frequency multiplier (harmonic generator) and a switched injection-locked oscillator as single stage pulsed high gain (> 50 dB) amplifier.

In this work, it is demonstrated that this approach allows synthesizing pulsed, arbitrarily phase modulated signals using the switched injection-locked harmonic sampling principle. The theory of this concept was investigated thoroughly and verified experimentally for the synthesis of phase shift keying (PSK) modulated communication signals and pulsed frequency modulated (PFM) radar signals with the same hardware. Regarding the switched

injection-locked oscillator, implementations in planar surface mounted technology (6-7, 7-8 GHz) and integrated circuits (6-8 GHz, 63 GHz) were developed. Measurements with the first designs confirm the feasibility of the proposed concepts and already show promising results regarding transmitter signal to spur ratio and achievable ranging resolution and ranging uncertainty.

This work shows the half-term results of the ongoing project “Components and concepts for low-power mm-wave pulsed angle modulated ultra wideband communication and ranging (PAMUCOR)” within the DFG priority programme “Ultra-Wideband Radio Technologies for Communications, Localization and Sensor Applications”; for comparison, some results from the previous project “Concepts and components for pulsed frequency modulated ultra wideband secondary radar systems (PFM-USR)” are summarized.

3. Pulsed angle modulated UWB signals

3.1. Signal definition

Fig. 1 depicts a pulsed angle modulated UWB signal consisting of a sequence of short pulses (width T_d , period T_s), in which each pulse is an oscillation with the frequency ω_{osc} and the modulated initial phase φ_i :

$$s(t) = \sum_{i=0}^N \cos \left(\omega_{osc} \left(t - i \cdot T_s + \frac{T_d}{2} \right) + \varphi_i \right) \cdot \text{rect} \left(\frac{t - i \cdot T_s}{T_d} \right) \quad (1)$$

with

$$\text{rect}(x) = \begin{cases} 1 & \text{for } -0.5 < x < 0.5 \\ 0 & \text{else} \end{cases}.$$

For flexible signal synthesis, initial phase modulation, pulse period, pulse width and oscillation frequency can be tuned.

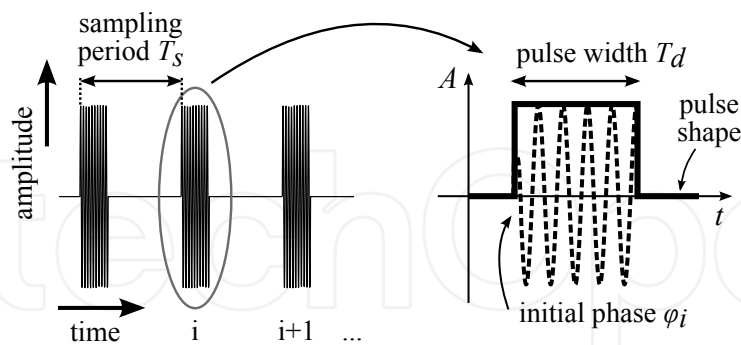


Figure 1. Pulsed angle modulated UWB signal - the modulated parameter is the initial phase φ_i of each pulse

3.2. SILO operation principle

The switched injection-locked oscillator (SILO) is basically a normal oscillator which is turned on and off while a weak reference signal is injected into its feedback loop (see Fig. 2). During startup of the oscillator, the injection signal provides an initial condition in the oscillator’s resonator instead of noise like in oscillators without injection signal. This way, the

instantaneous phase of the injection signal is adopted though the oscillator runs with its own natural frequency, which may differ from the injection signal's frequency. Since the power level of the injection signal is far too low to influence the oscillation as soon as the oscillator has reached its final amplitude, it performs only phase, but no frequency locking.

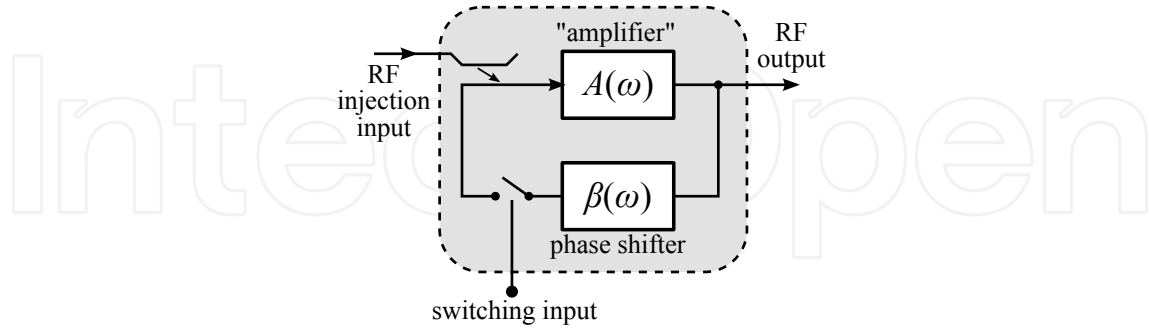


Figure 2. SILO principle

This behavior can be described theoretically by:

$$s(t) = \sum_{i=0}^N \cos \left(\omega_{osc} \left(t - i \cdot T_s + \frac{T_d}{2} \right) + \arg \{ s_{inj}(t) \} \right) \cdot \text{rect} \left(\frac{t - i \cdot T_s}{T_d} \right), \quad (2)$$

with the injection signal (center/reference frequency ω_{inj} , phase modulation $\varphi(t)$)

$$s_{inj}(t) = \cos \left(\omega_{inj} t + \varphi_{inj}(t) \right), \quad \arg \{ s_{inj}(t) \} = \omega_{inj} t + \varphi_{inj}(t). \quad (3)$$

In spite of the fact that this model only describes the fundamental principle, the physical behavior of the oscillator is very similar in most operation modes. The most important disregarded physical effects observed in real implementations are:

- Due to balancing imperfections e.g. in differential oscillators, high order harmonics of the startup pulse turning on the circuit cause self-locking effects that degrade the SILO's performance at low injection levels. Hence, the rise time of the oscillator should not be too short in order to reduce the harmonic power level. Obviously, this leads to a trade-off with spectral bandwidth, minimum pulse width and maximum achievable pulse repetition rate.
- The phase sampling process is affected by the amplitude of the injection signal. In consequence, amplitude variations of the injection signal are converted into phase distortions. Therefore, constant amplitude injection signals should be used to mitigate these effects. Then there is only a constant phase offset between injection and regenerated signal.
- If the rise time of the oscillator is configured to be relatively long compared to the pulse width, there will be a noticeable dependence between the injection signal's power level and pulse width. With a large amplitude injection signal, the oscillator settles much faster than when starting from noise level. Again, constant amplitude injection signals are the preferred countermeasure to avoid pulse width jitter.

Thus, the simplifications of the proposed ideal model mainly affect time and frequency domain amplitude shape, which makes this model suitable for the analysis of the phase sampling process.

3.3. Phase sampling theory

In [3, 4, 19], the SILO's phase sampling principle and its applications have been investigated thoroughly. The most important results will be summarized and discussed in the following.

Starting from equations (2) and (3), the SILO's output signal can be expressed by (disregarding negative frequencies and finite time domain waveform length for sake of simplicity):

$$s(t) = \sum_{i=-\infty}^{+\infty} \left[a \cdot e^{j(\omega_{osc}t + (\omega_{inj} - \omega_{osc}) \cdot (i \cdot T_s - \frac{T_d}{2}))} \cdot e^{j\varphi_{inj}(i \cdot T_s - \frac{T_d}{2})} \cdot \text{rect}\left(\frac{t - i \cdot T_s}{T_d}\right) \right]. \quad (4)$$

This expression still suggests an oscillation with ω_{osc} - the presence of the injection signal regeneration feature that includes the frequency is not obvious. According to [4], the Fourier transform $F\{\cdot\}$ of (4) leads to:

$$S(\omega) = A \cdot \left[\text{sinc}\left(\frac{(\omega - \omega_{osc}) \cdot T_d}{2}\right) \cdot \left(e^{j(\omega_{inj} - \omega_{osc}) \frac{T_d}{2}} \cdot F\{e^{j\varphi_{inj}(t - \frac{T_d}{2})}\}(\omega) * \delta(\omega - \omega_{inj}) * \text{III}_{\frac{1}{T_s}}\left(\frac{\omega}{2\pi}\right) \right) \right]. \quad (5)$$

The SILO output spectrum according to (5) consists of a convolution of the user-defined phase modulation spectrum with its center / carrier frequency signal and the sampling process' aliasing signal (Dirac comb, III), see Fig. 3. It is weighted with a sinc envelope centered at the oscillator's natural frequency ω_{osc} . Since this frequency only affects the envelope and a constant phase offset, the SILO can be regarded as a highly effective aliased regenerative amplifier. In consequence, an injected user-defined constant envelope phase modulated signal is reproduced correctly even with a free running oscillator with (in certain bounds) unknown natural frequency as long as Nyquist's sampling theorem is fulfilled (modulation bandwidth less than half pulse repetition frequency).

In general, this signal synthesis principle is not limited to phase modulated / constant envelope signal synthesis. For amplitude modulation, e.g. an electronically tuned attenuator at the SILO's output can be employed to manipulate the amplitude of each pulse synchronously to the pulse rate, which leads to a polar modulator. Since efficient pulse

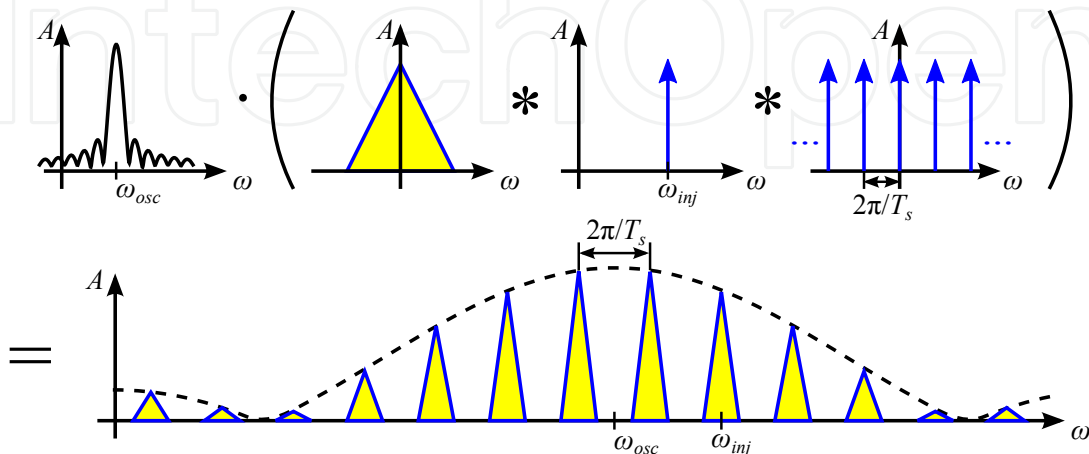


Figure 3. SILO output spectrum according to (5)

amplitude modulation is feasible for a long time in contrast to complex phase modulation and can be added independently, this work is concentrated on the latter aspect.

3.4. Phase modulated UWB communication signals

For the synthesis of communication signals [4], any phase modulated constant envelope signal that is bandwidth limited to half pulse repetition frequency can be chosen. The maximum possible symbol rate leads to one symbol per pulse.

Demodulation can be achieved similar to existing approaches that allow quadrature pulse demodulation (e.g. [11]). Basically, the phase of each pulse has to be sampled synchronously to the pulse sequence (i.e. during pulse duration), which can be realized e.g. by quadrature baseband down-conversion and synchronized sample acquisition. In this case, the sequence of received samples is given by

$$s_{recv}(k) = s(k \cdot T_s + \Delta t_{sync}) \cdot e^{-j\omega_{inj}(k \cdot T_s + \Delta t_{sync})}, \quad k \in \mathbb{N}, \quad (6)$$

where Δt_{sync} denotes a modestly (uncertainty less than half pulse width) unknown synchronization error that has to be taken into account in practice. Inserting (4) in (6) leads to:

$$s_{recv}(k) = A_r \cdot e^{j\left(\varphi_{inj}\left(i \cdot T_s - \frac{T_d}{2}\right) + (\omega_{osc} - \omega_{inj}) \cdot \left(\Delta t_{sync} + \frac{T_d}{2}\right)\right)}. \quad (7)$$

Accordingly, the original phase modulation φ_{inj} is reconstructed correctly aside from a constant phase offset. Its constancy is guaranteed as long as the natural frequency of the unstabilized oscillator does not drift too fast, which is mostly given due to relatively slow changes in environmental parameters like temperature. For compensation, e.g. differential modulation schemes or short frames can be applied.

3.5. Frequency modulated UWB radar signals

Since the SILO based synthesizer is capable of generating any constant envelope phase modulated signals (within the bandwidth limit), even a frequency modulated radar signal with the bandwidth B , sweep duration T and phase

$$\varphi_{inj,FM}(t) = 2\pi \frac{B}{2T} t^2 \quad (8)$$

can be transmitted. At the receiver, the time delayed transmit signal $s(t)$ is mixed with a FMCW signal:

$$s_{recv,FM}(t) = s(t - t_d) \cdot e^{-j(\omega_{inj}t + \pi \frac{B}{T} t^2)}. \quad (9)$$

According to [3], the approximate resulting beat frequency spectrum (disregarding envelope)

$$S_{recv,FM}(\omega) = \underline{A} \cdot \delta\left(\omega + 2\pi \frac{B}{T} \left(t_d + \frac{T_d}{2}\right)\right) * \text{III}_{\frac{1}{T_s}}(\omega) \quad (10)$$

is equivalent to the conventional FMCW spectrum except for the aliases resulting from switched operation and a constant phase offset \underline{A} . The (one way) distance can be calculated from

$$f_b = \frac{B}{T} \left(t_d + \frac{T_d}{2}\right) \quad (11)$$

given that transmitter and receiver were precisely synchronized, which can be achieved through two-way synchronization like in [16].

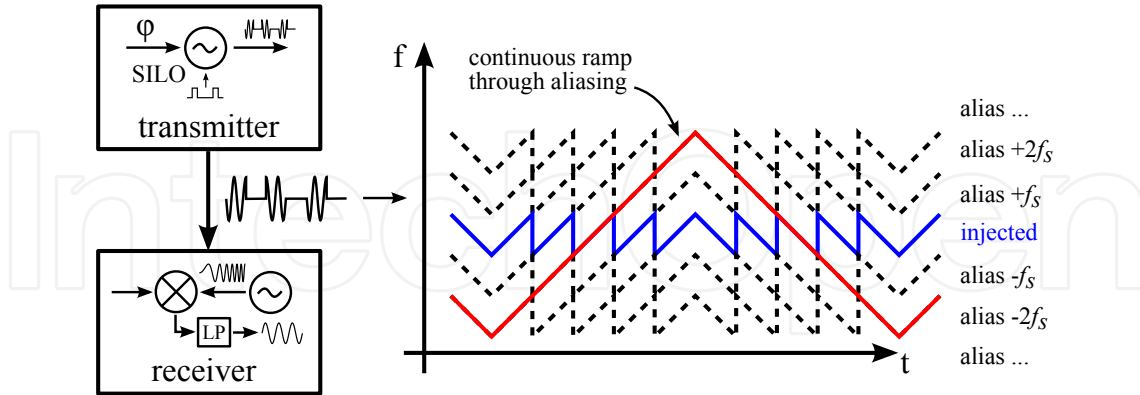


Figure 4. Exploiting sampling aliases to synthesize frequency modulated UWB radar signals with minimal effort

Strictly speaking, the sampling theorem is not met for a sweep bandwidth larger than the pulse repetition frequency. Though, aliasing can be exploited to minimize the ramp synthesis effort (see Fig. 4). The injected and regenerated signal is configured to represent a short chirp within the sampling bandwidth that is repeated continuously. Considering aliasing, the resulting signal appears to be continuous at the receiver when sweeping through all aliases.

The required effort can even be further reduced: Since the SILO only samples certain phase values, it is not necessary to actually generate continuous sweeps as intermediate signal. Instead, a CW injection signal with stepped phase modulation is sufficient as long as its phase (modulus 2π) equals (8) at sampling time. This approach results according to [3] in a short periodic sequence of samples (period $p \in \mathbb{N}^+$) under the condition that the term

$$\frac{pBT_s^2}{T} \quad (12)$$

is whole-number and p even. The sequence features a minimum period of

$$p_{min} = \frac{T}{BT_s^2}, \quad p_{min} \in \mathbb{N}^+. \quad (13)$$

The only restriction that results from exploiting aliases is a limitation in unambiguous range, i.e. maximum distance (phase velocity c_p):

$$d_{max} = \frac{c_p T}{BT_s}. \quad (14)$$

Considering a sampling period of 100 ns ($T_s = 10$ MHz), which is convenient for low power implementations, a sufficient maximum range of over 1 km can be achieved even at a high bandwidth of 2 GHz in 1 ms.

4. System concepts

In the following, concepts and implementations for the pulsed angle modulated signal synthesis principle are presented. Firstly, the harmonic sampling approach is presented,

which is used to take advantage of all benefits of the switched injection-locked oscillator concept by generating a high power, high frequency signal efficiently from a low frequency intermediate signal (4.1). Secondly, a frequency modulated direct digital synthesis (DDS) based upconversion approach for radar applications from the preceding project (PFM-USR) is presented as starting point for the subsequent development (4.2). Thirdly, the recent hardware concept and implementation for phase stepped modulation is described, which allows for synthesizing both frequency modulated radar signals and phase modulated communication signals with the same simple communication signal generator hardware for integrated communication and ranging.

4.1. Harmonic sampling approach

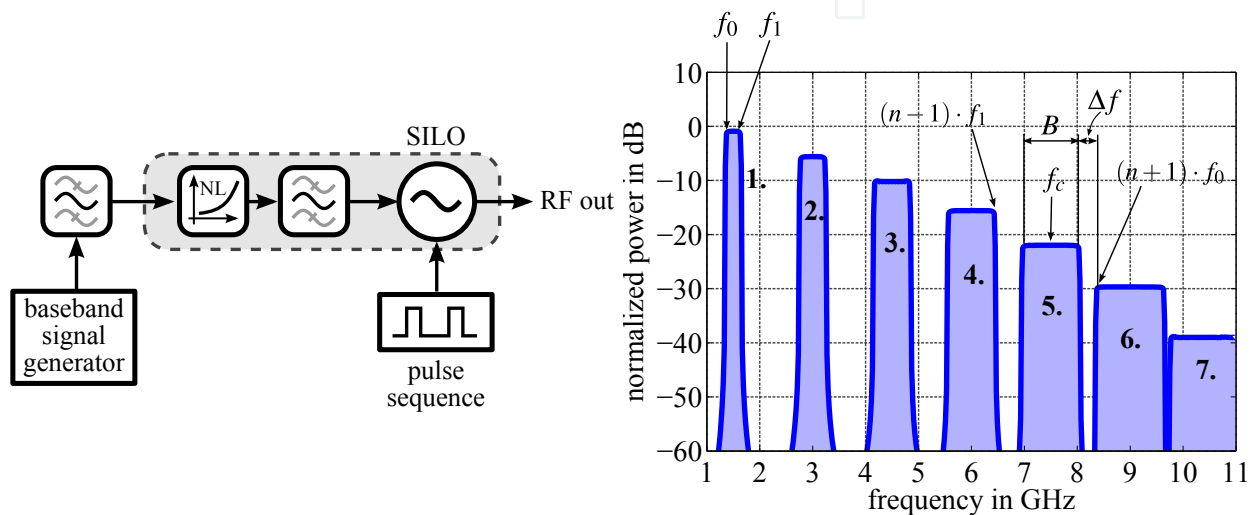


Figure 5. SILO based harmonic sampling; left: concept, right: spectrum of bandwidth limited signal after harmonic generator (here: FMCW sweep from f_0 to f_1) [2]

When synthesizing a high frequency pulsed angle modulated signal, classic approaches based on VCO, PLL, linear amplifier and pulsed switch are not suitable to meet goals like low complexity and low power hardware. Instead, a baseband modulator is proposed for signal generation that generates much lower frequencies than at the system's RF output, e.g. 5.8 GHz instead of 63.8 GHz. At lower frequency ranges, analog RF circuits are usually more efficient than their high frequency counterparts. The baseband signal is then applied to the input of a passive or low power non-linear element that generates harmonics, e.g. a diode or transistor (see Fig. 5). Finally, a SILO is used to amplify the upconverted signal by typically more than 50 dB (within pulse duration). Considering an instantaneous output power level of 0 to 5 dBm, an injection level of less than -45 dBm is sufficient, which allows for high losses and low power consumption in the preceding frequency multiplier stage.

In order to avoid strong intermodulation products caused by the baseband modulation, it should be "slow" compared to the center frequency of the baseband signal so that the non-linear element's instantaneous input and filtered output signal can be considered approximately single tone. This requirement is needed for the SILO, which can itself only correctly regenerate constant envelope signals (apart from the fact that intermodulation products are undesirable) that are stable during the startup phase of the oscillator, e.g. FMCW signals with low ramp slope or rectangular shaped PSK with symbol rate / pulse repetition frequency much smaller than RF frequency.

Regarding maximum baseband modulation bandwidth, there exists a limit for the frequency multiplication factor n in order to guarantee spectral separation, since the bandwidth increases with the harmonic order whereas the spacing of the harmonics' center frequencies is equidistant. According to [2] (see also Fig. 5 right), the upper boundary for the multiplication factor is (harmonic center frequency f_c , harmonic modulation bandwidth B):

$$n < \frac{f_c}{B} - \frac{1}{2}. \tag{15}$$

4.2. Frequency modulated baseband upconversion

The "classic" approach towards synthesizing linear frequency modulated signals (see Fig. 6) consists of a DDS generating a low frequency reference chirp, a PLL and VCO loop and a linear power amplifier. By adding a pulsed switch at the output, pulsed frequency modulation can be realized similar to section 4.2 as long as the pulse width is short enough (the latter signal has constant phase during the pulse, the first one features slight frequency modulation). Obviously, this classic approach has several disadvantages at high frequencies, especially power consuming linear amplifiers and a switch that dissipates more than 90% of the RF power at common pulse sequence duty cycles of less than 1:10.

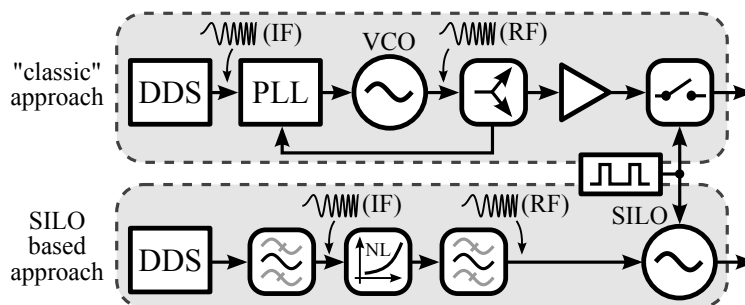


Figure 6. Comparison of classic and SILO based pulsed frequency modulated signal synthesis [2]

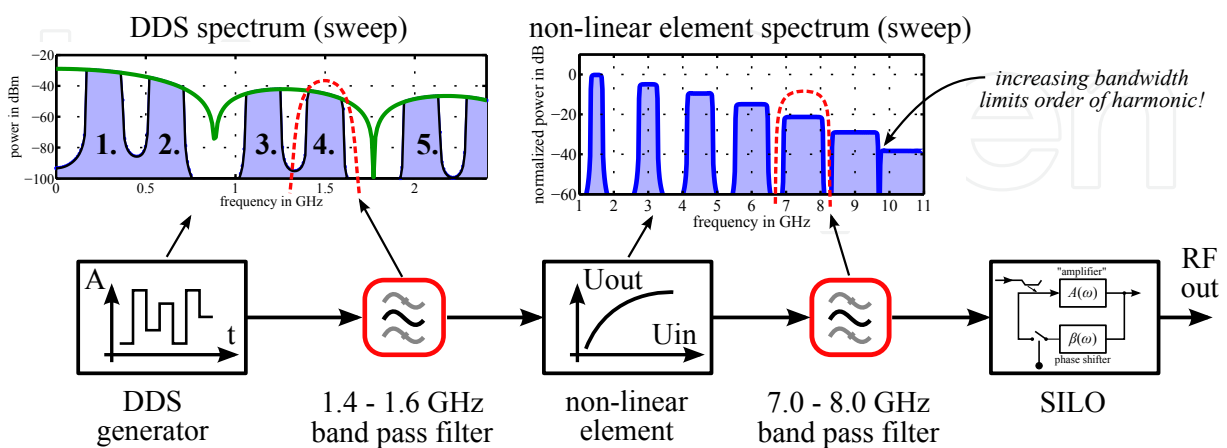


Figure 7. Harmonic sampling concept for FMCW baseband upconversion

Therefore, a harmonic sampling approach was proposed to directly synthesize the ramp from a DDS signal while avoiding PLLs and linear amplifiers at high frequencies [2]. Due to the

bandwidth restrictions with harmonic sampling (see section 4.1), a single non-linear stage is not sufficient to generate a 7-8 GHz ramp with a commercially available 1 GS/s DDS circuit. Hence, a Nyquist image from the DDS is used to shift the baseband output frequency range to 1.4-1.6 GHz (see Fig. 7).

The main advantage of this concept is that the generated pulsed frequency modulated signal features a very good linearity in comparison to simple PLL control loops and that the only active component at output frequency is a simple, efficient oscillator (SILO). Despite the simplicity of this concept, its hardware design is quite challenging, since the amplitude of a wideband sweep is subject to many inherent sources of frequency dependent amplitude behavior like DDS spectral envelope, insufficient filter flatness and the non-linear element, which increases existing amplitude variations notably.

4.3. Phase stepped modulation with CW baseband for integrating radar and communication

For integrated communication and ranging, it is desirable to construct a hardware that can synthesize signals for both domains. In the past, they have mostly been developed separately with different hardware concepts. The previously proposed concept (4.2) is well suited for radar systems, but very specific to frequency modulated signals. In fact, angle modulated communication signals can be synthesized with further reduced effort (see Fig. 8) from a CW source with a phase shifter. It is synchronized with the SILO's pulse sequence and its offset is configured to guarantee that each new phase state is stable when the oscillator is turned on. This kind of modulation technique can also be employed to generate frequency modulated signals efficiently according to section 3.5 by using an appropriate sequence of phase samples that represent a frequency chirp.

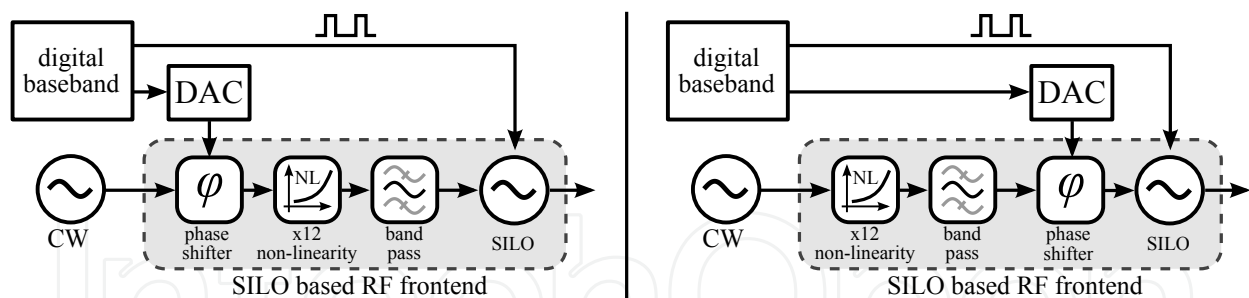


Figure 8. Concept for synthesizing pulsed angle modulated signals using a phase shifter; left: baseband phase modulation with 30 deg shifter, right: RF phase modulation with 360 deg shifter

Regarding hardware implementations, there are two major alternatives concerning the location of the phase shifter in the signal path. An attractive option is to add phase modulation before the frequency multiplication stage; this leads to a minimum amount of RF components and the phase shifter only needs to cover a shifting range of 30 degree, which is easy to design with good linearity. However, baseband modulation limits the multiplication factor (see section 4.1) and the phase shifter causes amplitude fluctuations that are increased in the subsequent non-linear stage. Alternatively, the phase shifter can be placed between RF filter and SILO, which allows for fast modulation, high multiplication factors with less effort (only a constant frequency single tone signal is applied), but requires a more sophisticated 360 degree phase shifter at RF frequency.

5. SILO concept and implementation

Consider the signal displayed in Fig. 1 and the basic SILO model depicted in Fig. 2. As a pulse width T_d of 1 ns and shorter was to be accomplished, the large parasitic capacitances associated with discrete components made it clear that only an integrated solution would be suitable for implementation of the SILO.

As a benchmark for the novel circuit concept of the SILO, some key components of a more conservative concept of generating pulsed frequency modulated signals were developed in an integrated circuit.

All integrated circuits were designed in Cadence Virtuoso and simulated using the Cadence Virtuoso Spectre Circuit Simulator (Cadence, Spectre and Virtuoso are registered trademarks of Cadence Design Systems, Inc). The transmission lines and passive baluns used in the 63.8 GHz-IC were simulated in the Sonnet Professional 2.5D field simulator.

5.1. The benchmark circuit: VCO with integrated switch

To evaluate the efficiency of the SILO approach, a conventional circuit using a VCO with wide tuning range and an output switch was designed. The system with the manufactured IC is shown in Fig. 9.

The schematic of the VCO can be seen in Fig. 10, together with the half-circuit of the designed output switch.

Parameter	$C_{var,min}^*$	$C_{var,max}^*$	$C_{var,min}$	$C_{var,max}$	L_B	R_E	R_{CC}
Value	65 fF	200 fF	145 fF	455 fF	0.41 nH	200 Ω	200 Ω
Parameter	C_1	C_2	C_3	C_4	V_{Bias}	V_{CC}	V_{tune}
Value	700 fF	200 fF	300 fF	300 fF	1.8 V	3.3 V	0 to 4 V

Table 1. VCO component parameters

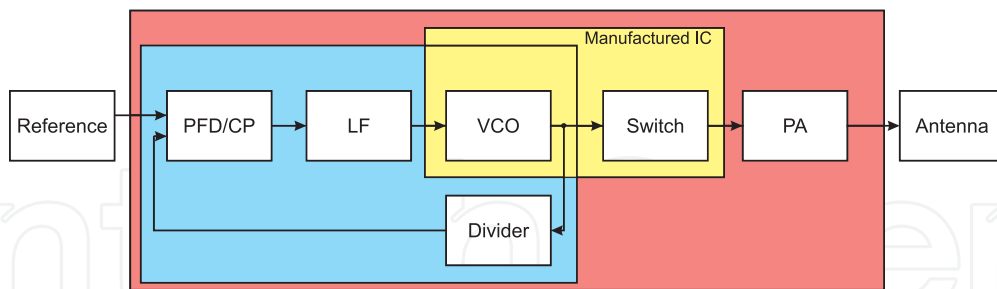


Figure 9. Pulsed frequency modulated continuous wave synthesizer system concept using an output switch

The VCO is based on a common collector Colpitts oscillator design, including a second varactor diode pair at the transistor base. It is described in detail in [8]. A short overview is given in the following.

A bipolar current mirror is used to drive the oscillator core. The emitter follower output buffer from [8] was replaced by a differential pair to increase common-mode rejection. The VCO frequency defining series resonant circuit consists of L_B and C_{in} :

$$f_{res} = \frac{1}{2\pi\sqrt{L_b C_{in}}} \quad (16)$$

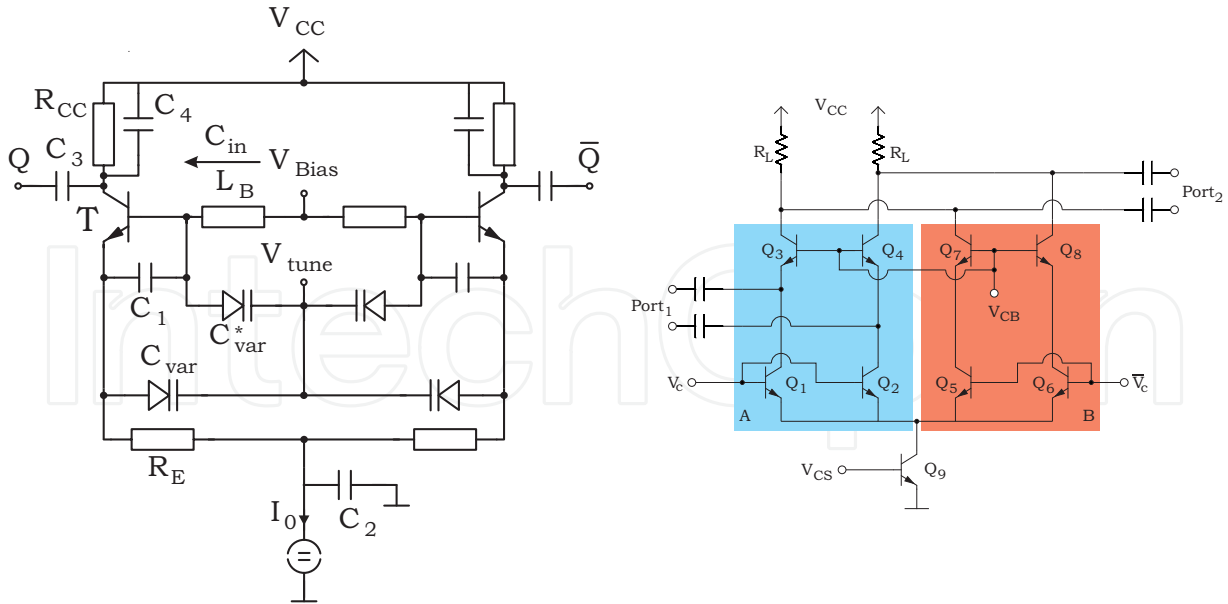


Figure 10. Synthesizer key components; left: VCO, right: half-circuit of single-pole double-throw switch

L_B is realized as a spiral inductor without tuning capability. Tuning is available by varying C_{in} , which has to be tuned over a wide tuning range using variable MOS-capacitance circuits.

For a minimum influence on the tuning range, C_P has to be minimized. It consists mainly of the collector base capacitance C_{CB} of transistor T and thus is given by size and bias conditions. C_S , which is determined mainly by C_{BE} , has to be maximized. Additionally, both varactor capacitance ranges have to be maximized. For a more detailed discussion, refer to [15]

The proposed pulsed ultra-wideband signal generation requires a switch after the frequency synthesizing PLL. The switch should have a minimum switching time in both on and off direction to enable the usage of very short pulses (in the 1 – 10 ns range). Additionally, a constant input port impedance is important in order not to change the loading of the oscillator.

A switch circuit was designed based on [10]. The original work was aimed at a 22 – 29 GHz UWB radar for automotive applications. Fig. 10, right, shows the half-circuit.

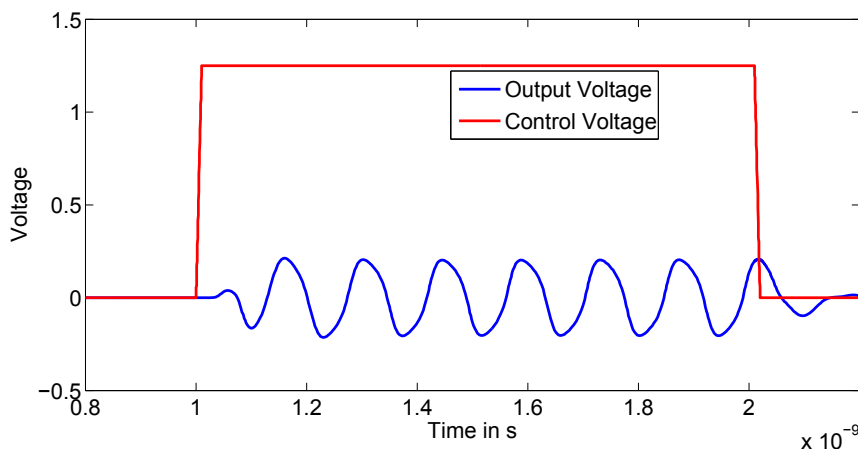


Figure 11. Switch transient simulation: Output voltage signal (blue) in reaction to control voltage (red) change.

The circuit works by switching the bias currents through branches A and B, implemented by transistors Q_1 to Q_4 and Q_5 to Q_8 , respectively. This is done by alternating the control voltages applied to switching stages Q_1/Q_2 and Q_5/Q_6 . The differential common base stages (Q_3/Q_4 and Q_7/Q_8) provide amplification and isolation, depending on the bias current. Transistor Q_9 provides the bias current, which is switched between the branches.

Fig. 11 shows the transient simulation of the output signal for a single rising V_C edge with a rise time of 5 ps. The delay between the control edge and a 90% of the output is below 250 ps. The addition of a matching network would improve insertion loss, but at the cost of worse area efficiency. The simulated input-referred noise was between $2.83 \text{ nV}/\sqrt{\text{Hz}}$ and $3.67 \text{ nV}/\sqrt{\text{Hz}}$.

A combination of VCO and output switch was simulated and then manufactured.

5.2. SILO oscillator concepts

As the injection locking property is universally stemming from oscillator theory, any oscillator can in theory be employed for switched-injection locking. There is an interesting trade-off to be made when considering an oscillator configuration for SILO building: The oscillator Q -factor should be high and excess loop gain should be low for better phase noise performance on the one hand, but a high- Q oscillator with low excess loop gain takes longer to begin oscillation, which is critical for pulsed angle modulated signal generation. A careful balance between the two qualities has to be found.

Another consideration has to be put into the point in the oscillator loop where the signal is injected into. In a cross-coupled oscillator, the resonator and gain stages are directly connected to the output. This means that there has to be a buffering circuit for the injected signal which provides backward isolation, in order to ensure the oscillation frequency of the oscillator is not influenced by the circuitry connected to the tank.

For the design of the SILO circuits, we concentrated on resonator-based oscillators, as they typically show better phase noise performance than inverter-based ring oscillators. A demonstrator implementation in discrete components was used for initial experimentation and verification of the viability of our approach. This circuit was aimed at a frequency range of 6 to 8 GHz. Subsequently, a SILO IC based on a pulse generator and a cross-coupled LC -oscillator was designed and manufactured. In a final step, a harmonics generator was combined with a Colpitts oscillator to sample a 5.8 GHz-signal and emit a 63.8 GHz-signal.

5.3. 6 and 8 GHz SMT SILO

For reference and for first experiments, SILO implementations based on surface mounted planar technology were realized. They are based on an ordinary common-collector Colpitts oscillator and designed for a natural frequency of 6 GHz respectively 7.5 GHz. In order to implement injection-locking, a directional coupler was added to apply the injection signal to the oscillator's output (see Fig. 12). The maximum achievable (10 dB) bandwidth is about 600 MHz at 7.5 ns pulse width.

Apart from parasitic technological limitations of lumped planar implementations, the single-ended design features an inherent source of self-locking to a harmonic of the switched power supply. Therefore, the pulse width is limited to about 10 to 20 ns in order to achieve a good compromise between bandwidth and minimum injection level. In consequence,

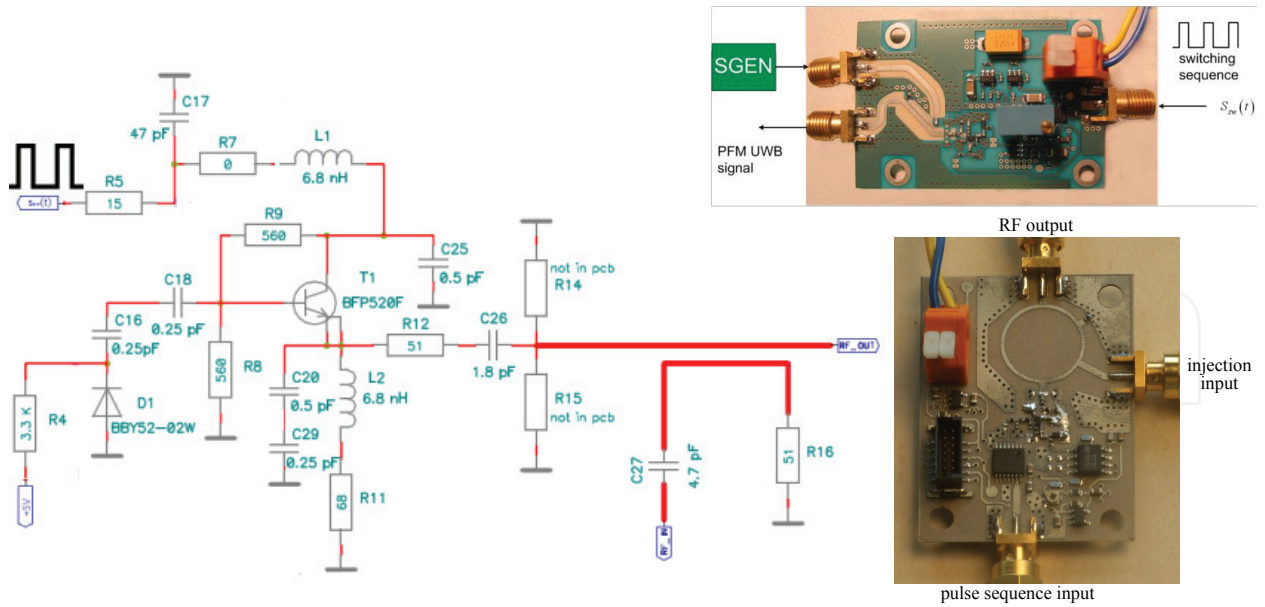


Figure 12. SILO SMT implementation; left: schematic of 7.5 GHz version; upper right: 7.5 GHz implementation; lower right: 6 GHz implementation

differential integrated circuit implementations are expected to deliver a significantly better self-locking suppression allowing much shorter pulsed in the order of 1 ns with comparable performance.

5.4. 7 GHz integrated circuit

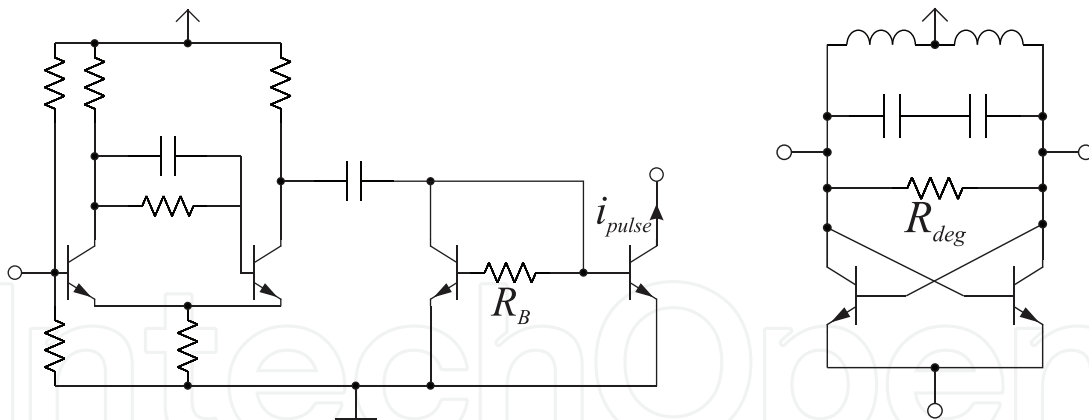


Figure 13. 7 GHz SILO circuits; left: Schmitt-trigger with peak generator, right: VCO with Q-degeneration resistor

The circuit consists of two active baluns for single-ended to differential and differential to single-ended conversion, a Schmitt-trigger with modified current mirror load for current peak generation and a simple cross-coupled oscillator for signal generation. It has an externally controllable pulse repetition rate and a pulse duration of approx. 1 ns. During operation it consumes 33 mA at 3.3 V supply voltage, while generating a $> 330 \text{ mV}_{pp}$ signal. The generated signal has a 10 dB-bandwidth of over 2 GHz at 7.5 GHz center frequency.

Both Schmitt trigger with current peak generator and VCO with Q-degeneration circuits are shown in Fig. 13.

As efficient integrated circuits are built in a differential configuration but external circuitry and measurement equipment usually are only available in single-ended configuration, single-ended to differential (S2D) and differential to single-ended (D2S) conversion circuits are needed in the IC. We designed a simple active balun circuit that can act as both S2D-and D2S-converter. When employed as a S2D-converter, both outputs and one input are connected, when used as a D2S-converter, one output and both inputs are connected.

In order to control the pulse repetition rate externally, a Schmitt-trigger circuit with current peak generator was designed based on [13]. The circuit enables a wide variety of pulse repetition rates (1 – 80 MHz could be achieved with the measurement equipment at hand). The resistor R_B together with base-emitter capacitance C_{BE3} controls the time constant $\tau_{current}$ of the charging circuit:

$$\tau_{current} = R_B C_{BE3}. \quad (17)$$

The peak generator was designed for a pulse duration of 1 ns by selecting the size of the resistor $R_B = 5 \text{ k}\Omega$.

For the oscillator, a simple cross-coupled topology was chosen. As the oscillator has to lock to the injected phase, a low Q is preferable. In order to degenerate the Q , a resistor was connected in parallel to the LC -tank circuit. The current is provided by the peak generator. Fig. 13 shows the implementation.

A simple common-collector circuit is used as an output buffer to drive the 50Ω load.

5.5. 63 GHz integrated circuit

The system developed for pulsed angle modulated signal generation at mm-wave frequency is shown in Fig. 14. The input signal of 5.8 GHz is coupled into the harmonics generator, which consists of a bipolar transistor with a resonant load. The load consisting of a transmission line of inductance L_1 and capacitors C_1 and C_2 is designed to couple the wanted 11th harmonic into the transformer. Fig. 17 shows the output power for the 1st, 10th, 11th and 12th harmonic depending on the input power. For an input power $> -3 \text{ dBm}$, the 11th harmonic is the strongest. The now differential signal is used to lock the VCO shown in Fig. 15.

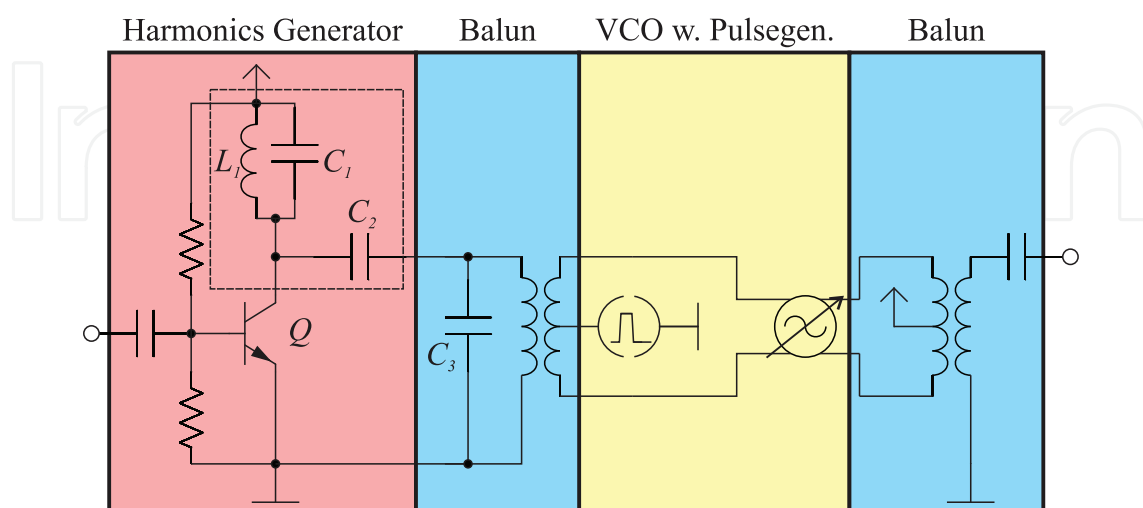


Figure 14. 63 GHz-system consisting of harmonics generator, baluns and VCO with pulse generator

The signal is coupled to the collector load transmission lines of the Colpitts oscillator using a transformer with a center tap. The center tap is connected to the pulsed current source of the oscillator.

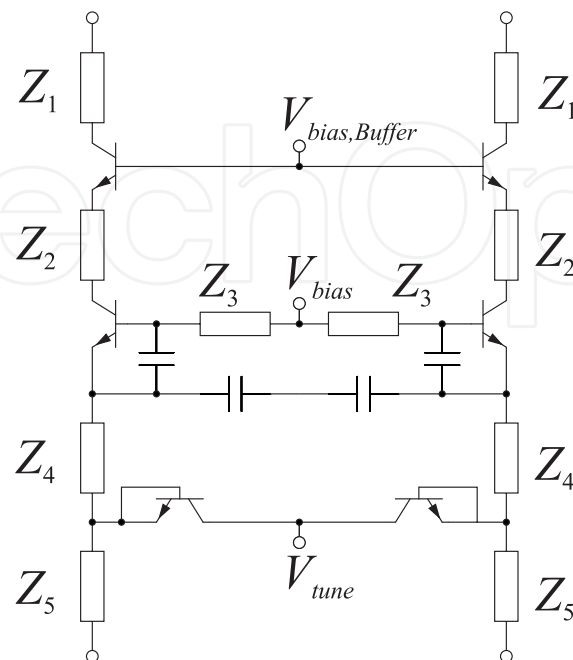


Figure 15. 63.8 GHz Colpitts voltage controlled oscillator schematic. Z_1 to Z_5 denote transmission lines

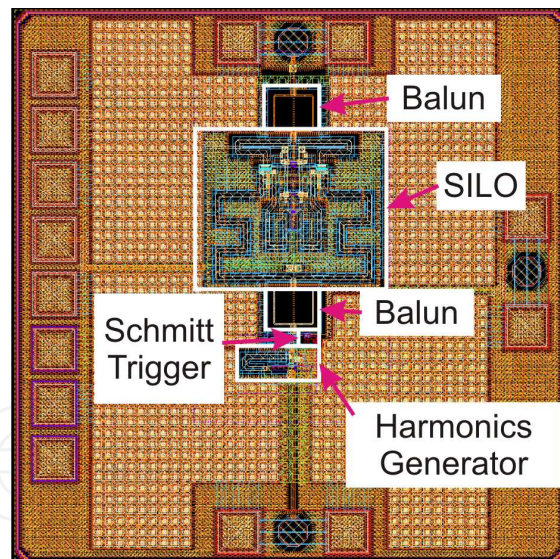


Figure 16. Layout of 63.8 GHz SILO

The simulation of the whole system was not possible. This is due to the fact that the system works in three frequency ranges, which differ by the order of magnitudes: The 5.8 GHz input signal, the 63.8 GHz output signal and the SILO pulse repetition frequency (10 – 100 MHz). Combined with the unknown modeling of switched injection-locking in the EDA software made it more viable to design each component (harmonics generator, VCO, pulse generator) separately. 16 shows the layout of the SILO circuit with its sub-components.

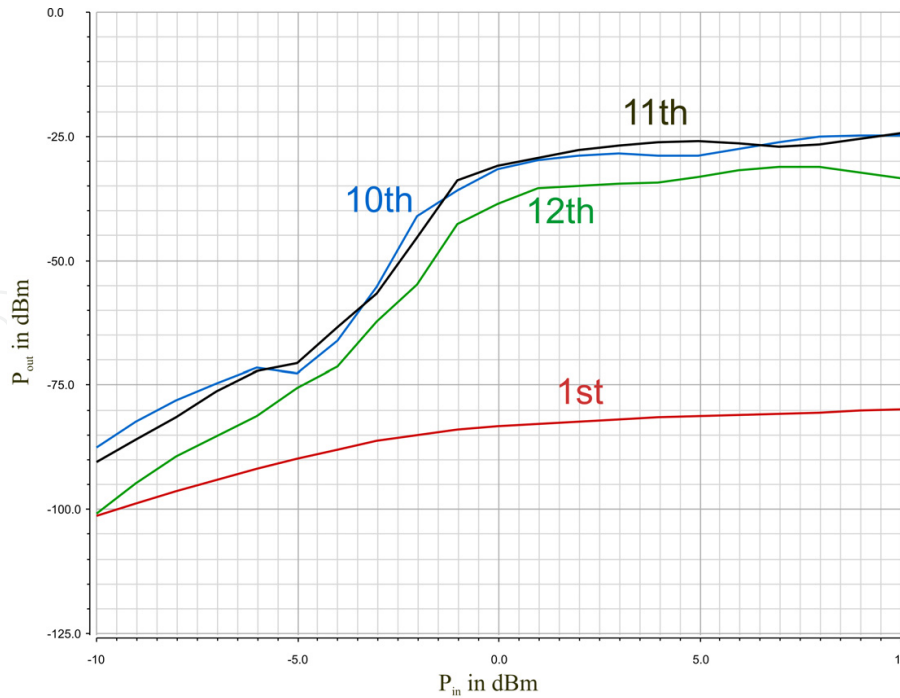


Figure 17. Power of the generated harmonics over the input power of the harmonics generator

6. Measurement setup and results

6.1. Verification of sampling theory

In order to verify the theoretical predictions concerning the switched injection locked harmonic sampling approach according to section 3.3, a demonstrator based on lumped planar components was built (see Fig. 18 and 19). It consists of a 480 MHz, 0 dBm signal source, a 10 MHz DAC modulated phase shifter, a single biased bipolar transistor frequency multiplier, a band pass filter (200 MHz @ 5.8 GHz) and the 5.8 GHz switched injection locked oscillator, which is turned on and off by the digital baseband synchronously to DAC modulation. Fig. 20 depicts the spectrum at the SILO's output. It features the typical sinc shaped peak comb in pulsed mode, which is aligned to and follows the injection frequency of 5.76 GHz when changed. When tuning the oscillators natural frequency (which is according to Fig. (20) different from the injection frequency) using a varactor diode, the sinc shape of the spectrum moves on the frequency axis while the peak positions do not change. These results prove most of the main claims of the generalized sampling theory according to (5) [4].

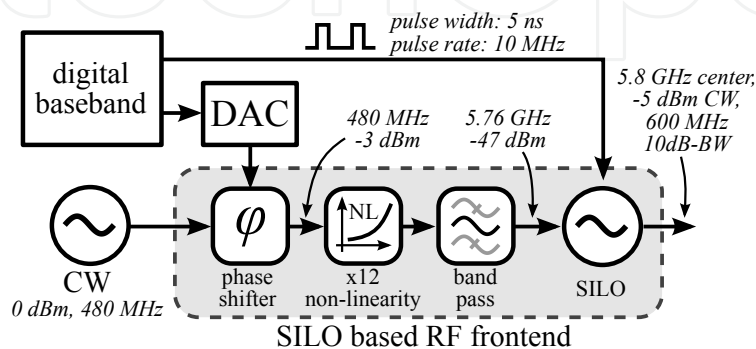


Figure 18. Implementation of communication and radar signal generator [4]

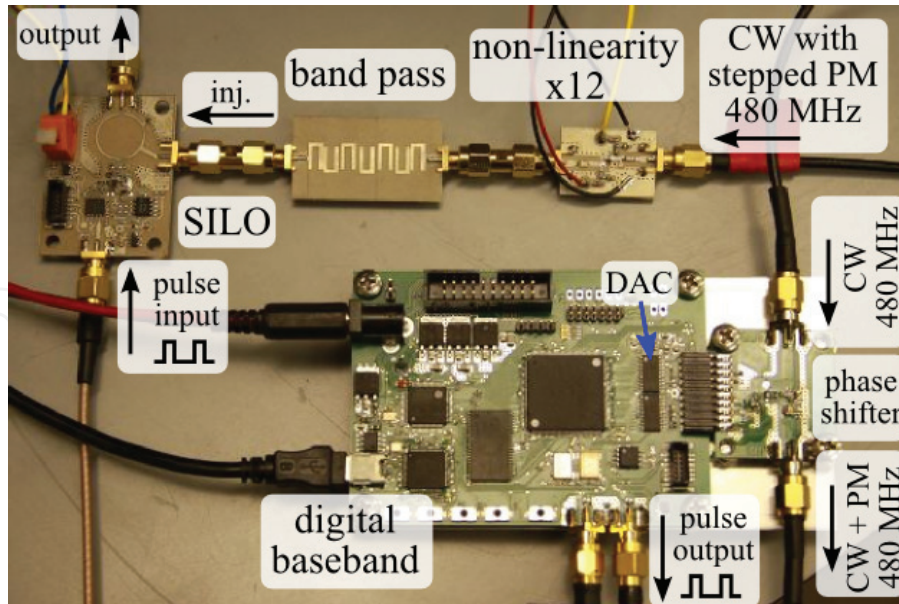


Figure 19. Hardware components for the 6 GHz transmitter system demonstrator (using lumped planar components SILO implementation)

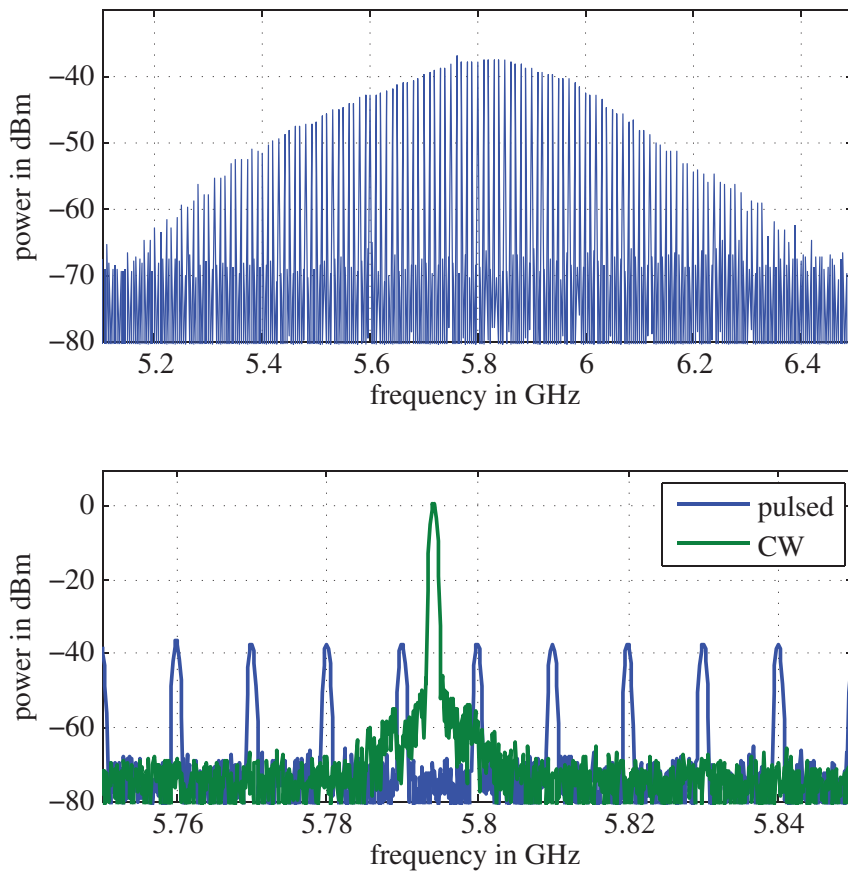


Figure 20. Spectrum of SILO based demonstrator with CW modulation; large peak: oscillator permanently on, comb: pulsed oscillator, background: comb zoomed out to show envelope, span 1.5 GHz [4]

6.2. Synthesis of communication signals

The synthesis of time domain communication signals was demonstrated using an 8 PSK modulation with cyclic transmission of all symbol values and maximum symbol rate, i.e. one symbol per pulse. The output signal of the demonstrator (Fig. 18, 19) was mixed to baseband using a quadrature mixer and displayed using an oscilloscope. Its waveform (Fig. 21) clearly shows the phase states and their repeatability in the IQ diagram. These results prove for the first time that it is feasible to generate UWB signals with more complex phase modulation than BPSK while at the same time keeping complexity and power consumption low.

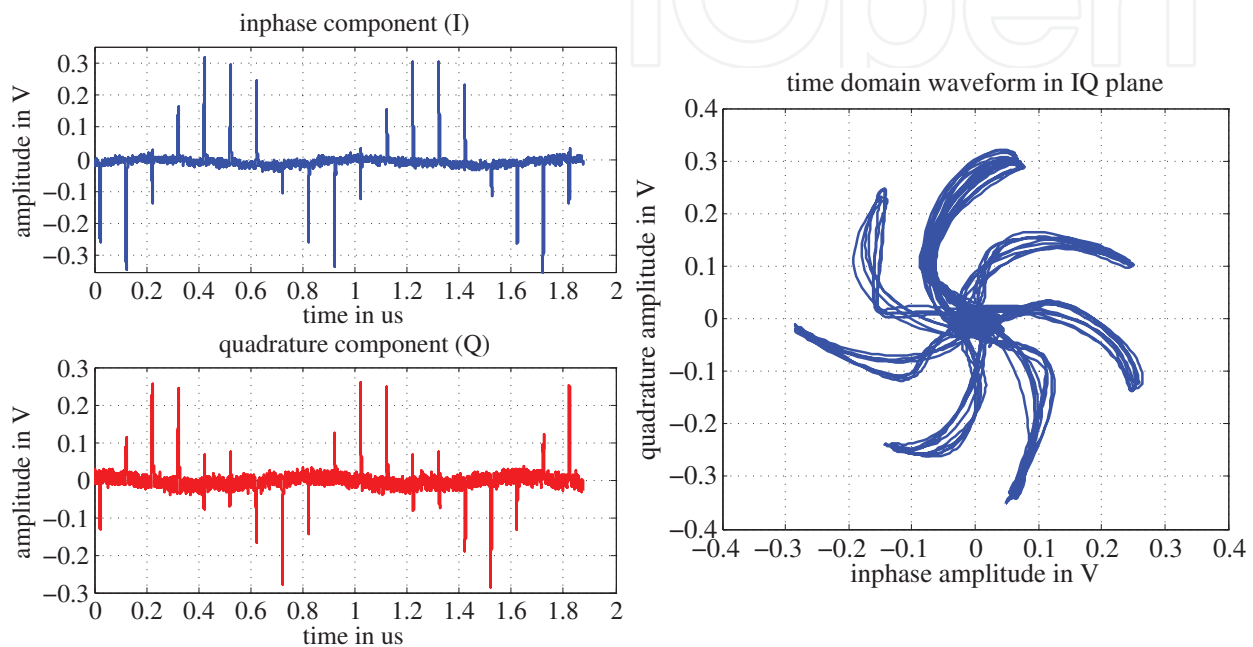


Figure 21. Generator output with 8 PSK modulation mixed to DC; left: inphase and quadrature component, right: IQ diagram [4]

6.3. Synthesis of radar signals

According to sections 3.5 and 4.3, the same simple hardware implementation used for communication signal synthesis (Fig. (18), (19)) can be employed to generate pulsed frequency modulated radar signals by repeatedly transmitting a limited list of phase samples. For a pulse rate of 10 MHz and a ramp slope of 20 MHz/ μ s, only 50 phase samples (one per pulse) are sufficient.

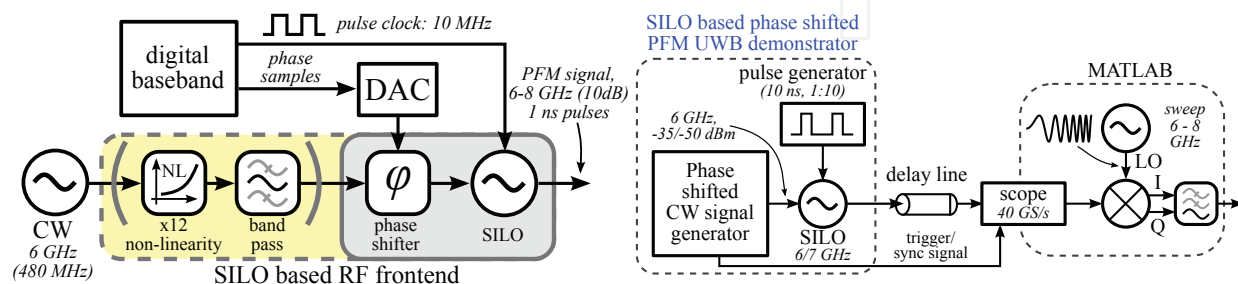


Figure 22. Measurement setup (on-waver) for the synthesis of radar signals using an integrated circuit SILO [3]

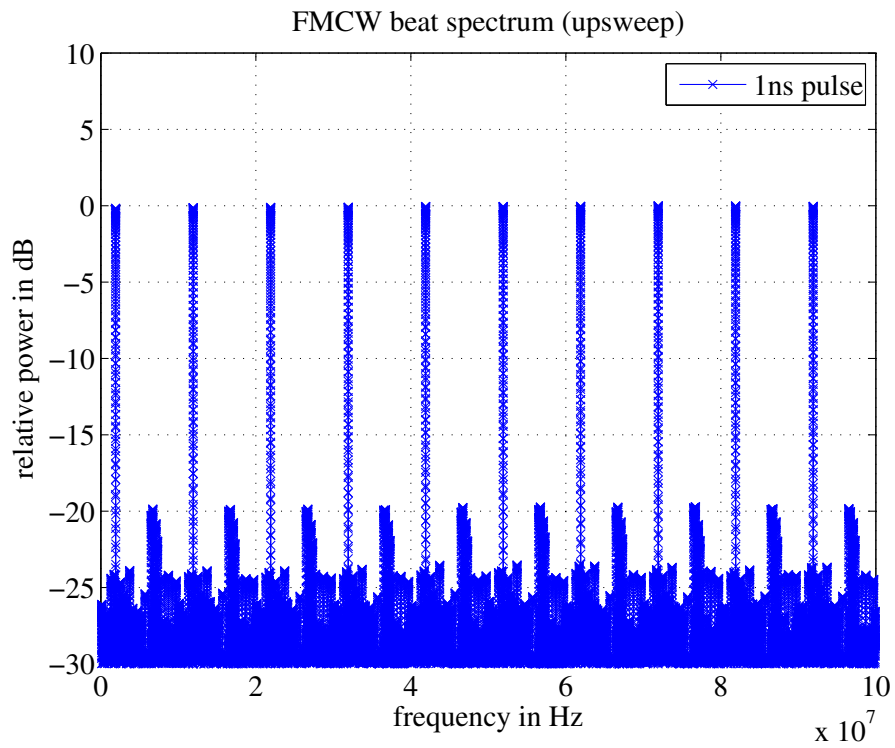


Figure 23. Beat spectrum (6-8 GHz SILO chip) of measured radar signal after mixing with linear sweep and before low pass filtering [3]

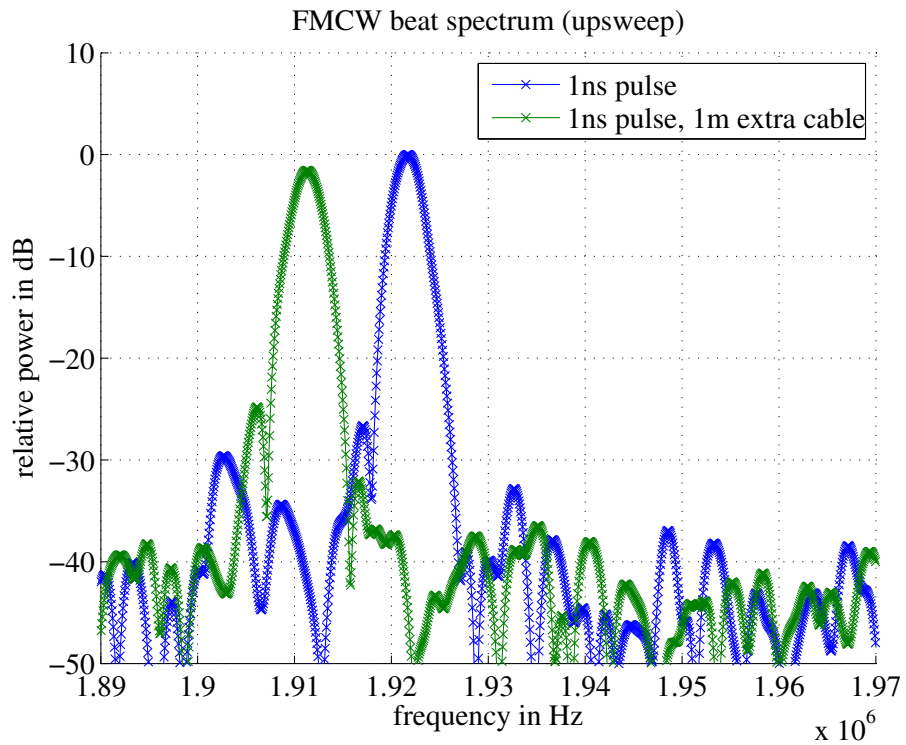


Figure 24. Zoomed beat spectrum (6-8 GHz SILO chip), comparison of two waveforms with different transmission delays [3]

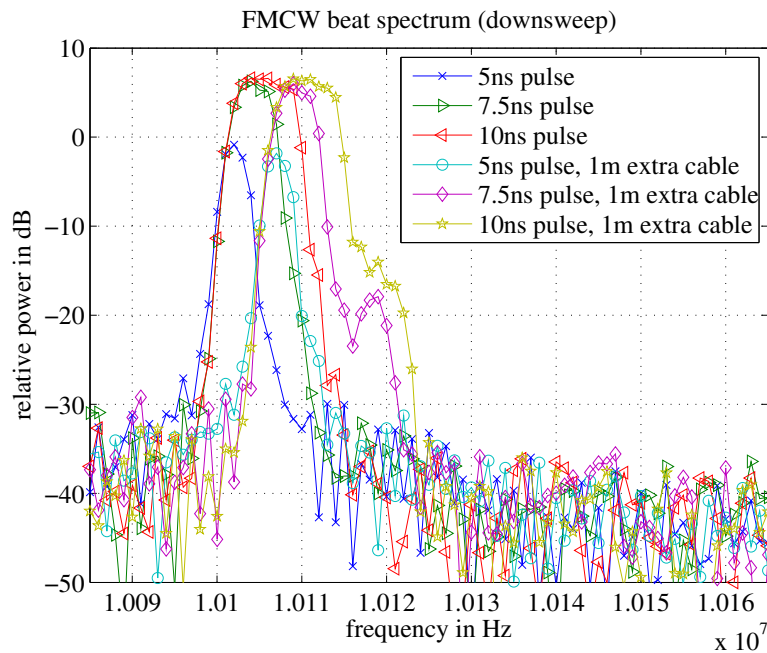


Figure 25. Comparison of 6-8 GHz chip (2 GHz bandwidth) with lumped implementation (wider pulses, smaller bandwidth) [3]

For verification, this approach was realized both using the previously employed lumped components SILO (6 GHz, 600 MHz bandwidth) and the first large bandwidth integrated circuit implementations (7 GHz, >2 GHz bandwidth) in order to demonstrate the resolution benefit for ranging. The setup for both experiments is depicted in Fig. 22; the generated and delayed signal is acquired using an oscilloscope and evaluated on a PC using a numerical computation software where it is mixed with a linear FMCW signal and analyzed in frequency domain (FFT).

Fig. 23 and 24 show the resulting beat frequency spectrum for the integrated circuit implementation using 1 ns pulses and 10 MHz pulse repetition rate. It corresponds to equation (10) except the small peaks that result from imperfections in the oscillator design leading to a slight turn-on pulse self-locking effect. Future designs are expected to fix this issue.

Comparing the results of the lumped and integrated circuit implementations (see Fig. 25), the benefit of much higher bandwidths regarding resolution becomes obvious. If the oscillator's spectral bandwidth is too small in relation to the sweep bandwidth, the beat frequency peak is broadened because of additional windowing through the narrowband SILO spectrum. Therefore, the oscillator bandwidth / pulse width should be adjusted to the desired sweep bandwidth in order to maximize spectral efficiency [3].

6.4. VCO with switch IC

The manufactured circuit is depicted in Fig.26. It measures $710 \times 1455 \mu\text{m}^2$. For reasons of nonavailability of differential equipment, all measurements were done single-ended with the unused output terminated to ground with a 50Ω resistor.

Fig. 27 shows the output power over the tuning range. The 10 dB decrease of output power compared to the previously published [8] VCO is attributed to the different VCO output buffer and the insertion loss of the switch.

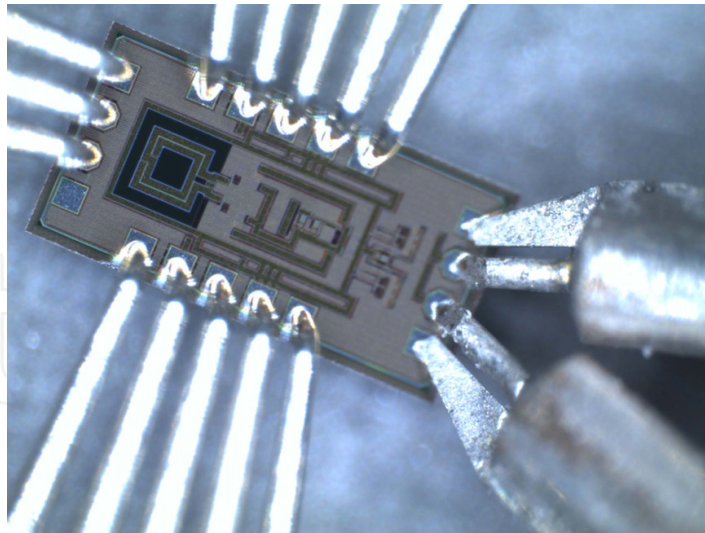


Figure 26. VCO with switch circuit IC photograph

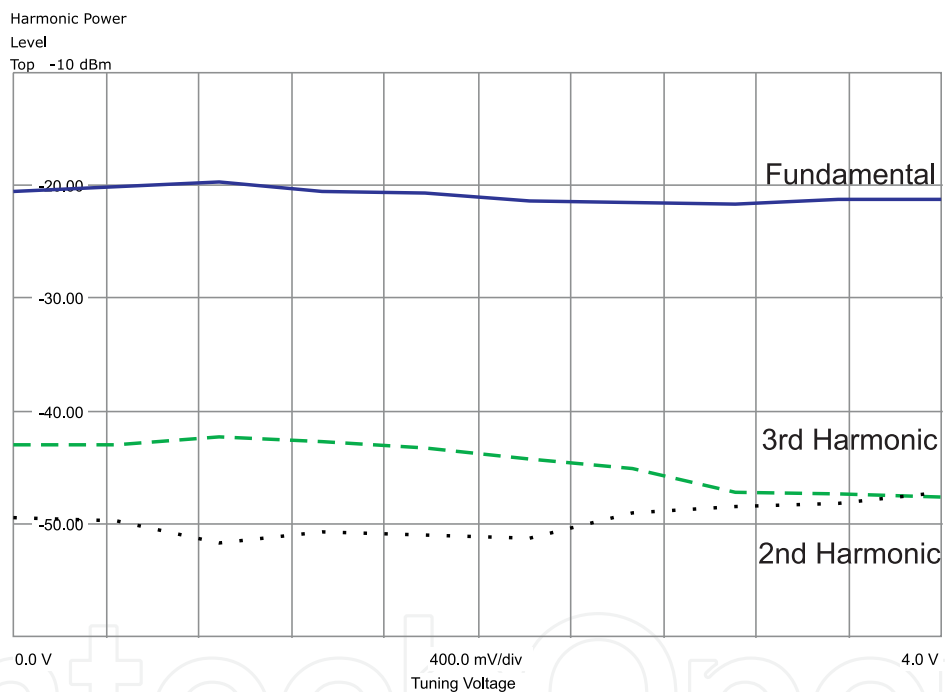


Figure 27. Measured output power of 1st, 2nd and 3rd harmonic of VCO with switch

The phase noise performance of the VCO with switch has deteriorated significantly from the previous [8] stand-alone VCO. This is mainly attributed to the new buffer structure which performed worse than anticipated.

6.5. 7 GHz SILO IC

The IHP Technologies SGB25V 250 nm SiGe:C BiCMOS process was chosen for manufacturing. It provides a cheap and flexible platform including one or two thick top metal layers consisting of aluminum. The advantage of using a BiCMOS process for a transmitter circuit is the possibility to build a system-on-a-chip (SoC) solution that integrates

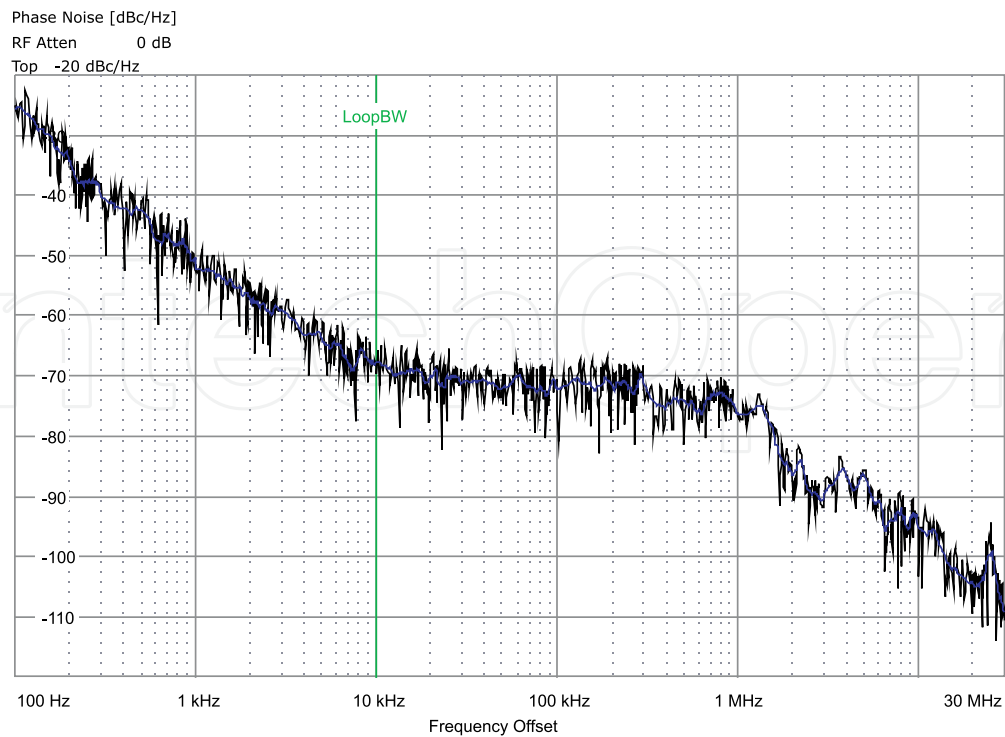


Figure 28. Measured phase noise of VCO with switch circuit

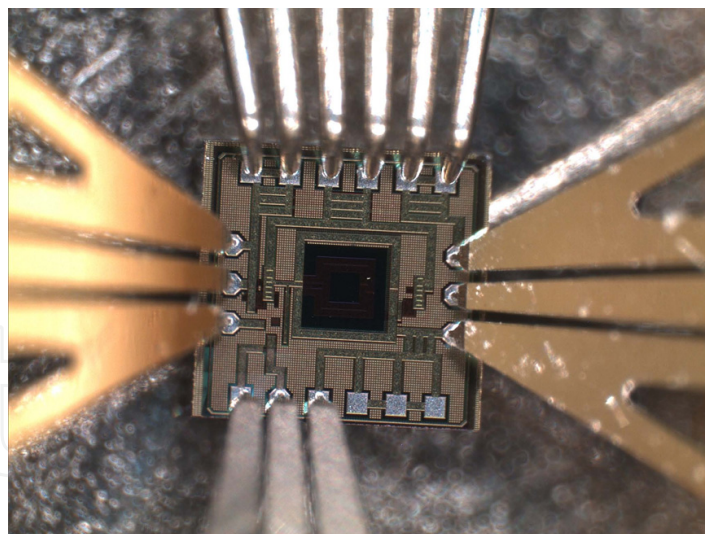


Figure 29. Manufactured 7GHz SILO IC

digital baseband and analog RF circuits. Fig. 29 shows a chip photograph with connected measurement probes.

Fig. 30 shows the output power spectrum of the manufactured SILO.

The 10 dB-bandwidth stretches from 5 to 8 GHz. A single pulse is shown in Fig. 31. A single cycle of oscillator start up, oscillation and decay has a duration of 1.5 ns.

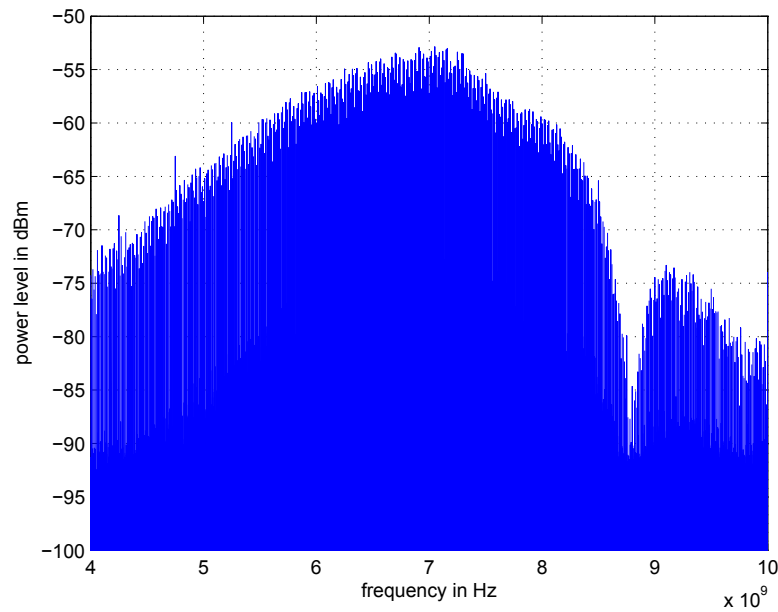


Figure 30. Measured output spectrum of 7 GHz SILO IC

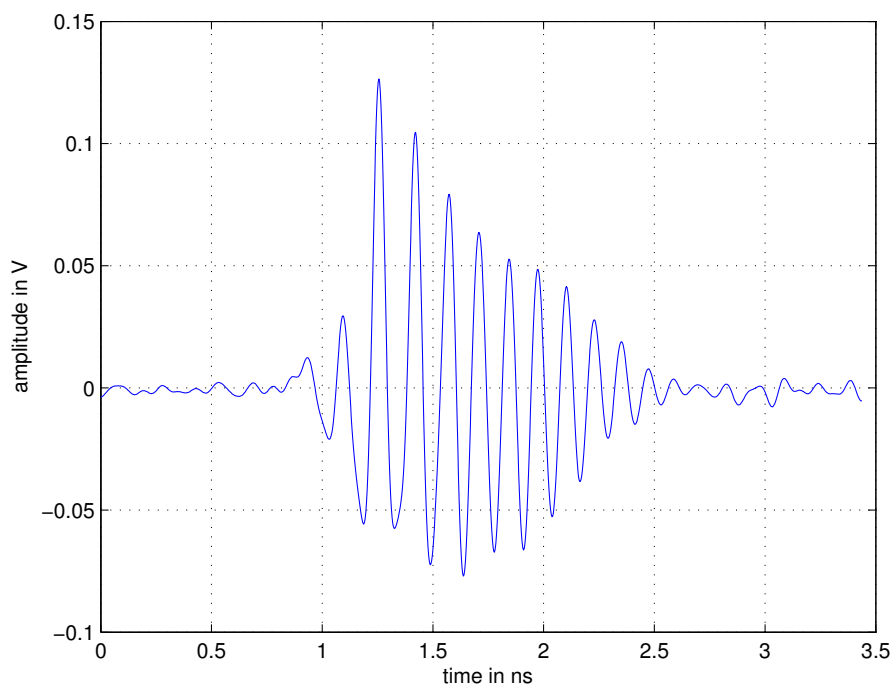


Figure 31. Transient output of 7 GHz SILO IC

7. Future work

Since this project is still ongoing, future work will cover further aspects that enhance theory and hardware implementation. Regarding pulsed angle modulated signals, more complex modulation schemes will be developed in conjunction with a more comprehensive study of error sources and their compensation. Furthermore, the first designs of the SILO circuit will

be refined for an even better performance and higher integration level. Last but not least, hardware concepts for receiver technology are being developed.

Acknowledgement

This work was supported by the German Research Foundation (DFG - priority program SPP1202, grant VO 1453/3-2) within the project “Components and concepts for low-power mm-wave pulsed angle modulated ultra wideband communication and ranging”.

Author details

Alexander Esswein and Robert Weigel

Institute for Electronics Engineering, University of Erlangen-Nuremberg, Germany

Christian Carlowitz and Martin Vossiek

Institute of Microwaves and Photonics, University of Erlangen-Nuremberg, Germany

8. References

- [1] Barrett, T. W. [2000]. History of UltraWideBand (UWB) Radar & Communications: Pioneers and Innovators.
- [2] Carlowitz, C., Esswein, A., Weigel, R. & Vossiek, M. [2012a]. A low power Pulse Frequency Modulated UWB radar transmitter concept based on switched injection locked harmonic sampling, *Microwave Conference (GeMiC), 2012 The 7th German*, pp. 1–4.
- [3] Carlowitz, C., Esswein, A., Weigel, R. & Vossiek, M. [2012b]. Synthesis of Pulsed Frequency Modulated Ultra Wideband Radar Signals Based on Stepped Phase Shifting, *IEEE International Conference on Ultra-Wideband (ICUWB)*.
- [4] Carlowitz, C. & Vossiek, M. [2012]. Synthesis of Angle Modulated Ultra Wideband Signals Based on Regenerative Sampling, *IEEE International Microwave Symposium 2012*.
- [5] Chandrakasan, A., Lee, F., Wentzloff, D., Sze, V., Ginsburg, B., Mercier, P., Daly, D. & Blazquez, R. [2009]. Low-Power Impulse UWB Architectures and Circuits, *Proceedings of the IEEE* 97(2): 332–352.
- [6] Deparis, N., Loyez, C., Rolland, N. & Rolland, P.-A. [2008]. UWB in Millimeter Wave Band With Pulsed ILO, *Circuits and Systems II: Express Briefs, IEEE Transactions on* 55(4): 339–343.
- [7] Deparis, N., Siligarisy, A., Vincent, P. & Rolland, N. [2009]. A 2 pJ/bit pulsed ILO UWB transmitter at 60 GHz in 65-nm CMOS-SOI, *Ultra-Wideband, 2009. ICUWB 2009. IEEE International Conference on*, pp. 113–117.
- [8] Esswein, A., Dehm-Andone, G., Weigel, R., Aleksieieva, A. & Vossiek, M. [2010]. A low phase-noise SiGe Colpitts VCO with wide tuning range for UWB applications, *Wireless Technology Conference (EuWIT), 2010 European*, pp. 229–232.
- [9] Grass, E., Siaud, I., Glisic, S., Ehrig, M., Sun, Y., Lehmann, J., Hamon, M., Ulmer-Moll, A., Pagani, P., Kraemer, R. & Scheytt, C. [2008]. Asymmetric dual-band UWB / 60 GHz demonstrator, *Personal, Indoor and Mobile Radio Communications, 2008. PIMRC 2008. IEEE 19th International Symposium on*, pp. 1–6.
- [10] Hancock, T. & Rebeiz, G. [2005]. Design and Analysis of a 70-ps SiGe Differential RF Switch, *Microwave Theory and Techniques, IEEE Transactions on* 53(7): 2403–2410.

- [11] J. Ryckaert et al [2006]. A 16mA UWB 3-to-5GHz 20Mpulses/s Quadrature Analog Correlation Receiver in 0.18/ μm CMOS, *Solid-State Circuits Conference, 2006. ISSCC 2006. Digest of Technical Papers. IEEE International*, pp. 368–377.
- [12] Kohno, R. [2008]. Latest regulation and R&D for UWB inter-vehicle radar in millimeter wave band, *8th International Conference on ITS Telecommunications, ITST* .
- [13] Lin, D., Schleicher, B., Trasser, A. & Schumacher, H. [2011]. Si/SiGe HBT UWB impulse generator tunable to FCC, ECC and Japanese spectral masks, *Radio and Wireless Symposium (RWS), 2011 IEEE*, pp. 66–69.
- [14] Miesen, R., Ebelt, R., Kirsch, F., Schaefer, T., Li, G., Wang, H. & Vossiek, M. [2011]. Where is the Tag? History, Modern Concepts, and Applications of Locatable RFIDs, *IEEE Microwave Magazine* . to be published.
- [15] Pohl, N., Rein, H.-M., Musch, T., Aufinger, K. & Hausner, J. [2009]. SiGe Bipolar VCO With Ultra-Wide Tuning Range at 80 GHz Center Frequency, *44(10)*: 2655–2662.
- [16] Roehr, S., Gulden, P. & Vossiek, M. [2008]. Precise Distance and Velocity Measurement for Real Time Locating Using a Frequency Modulated Continuous Wave Secondary Radar Approach, *IEEE Transactions on Microwave Theory and Techniques* *56(10)*: 2329–2339.
- [17] Sewiolo, B., Hartmann, M., Guenther, O. & Weigel, R. [2006]. System Simulation of a 79 GHz UWB-Pulse Radar Transceiver Front-End for Automotive Applications, *VDE / ITG Diskussionssitzung Antennen und Messverfahren fuer Ultra-Wide-Band(UWB)-Systeme (UWB 2006) Kamp-Lintfort, Germany* .
- [18] Trotta, S., Dehlink, B., Knapp, H., Aufinger, K., Meister, T., Bock, J., Simburger, W. & Scholtz, A. [2007]. SiGe Circuits for Spread Spectrum Automotive Radar, *Ultra-Wideband, 2007. ICUWB 2007. IEEE International Conference on*, pp. 523–528.
- [19] Vossiek, M. & Gulden, P. [2008]. The Switched Injection-Locked Oscillator: A Novel Versatile Concept for Wireless Transponder and Localization Systems, *Microwave Theory and Techniques, IEEE Transactions on* *56(4)*: 859–866.
- [20] Wentzloff, D. & Chandrakasan, A. [2006]. Gaussian pulse Generators for subbanded ultra-wideband transmitters, *Microwave Theory and Techniques, IEEE Transactions on* *54(4)*: 1647–1655.